Grain Size Hardening in Mg and Mg-Zn Solid Solutions

C.H. CACERES, GEMMA E. MANN, and J.R. GRIFFITHS

Cast specimens of Mg and of several Mg-Zn binary alloys with a wide range of grain sizes were deformed in tension and compression. The k values calculated from the Hall–Petch (H-P) plots of the tensile 0.2 pct proof stress increased with the Zn content, from 0.24 MPa $m^{1/2}$ for pure Mg to ~0.66 MPa $m^{1/2}$ for the 2.3 at. pct Zn alloy; k values measured from compression tests were larger, typically by 0.05 MPa $m^{1/2}$. When the strength measurements were corrected for the pseudoelastic strain resulting from elastic twinning, the k values generally increased, and the difference between tension and compression was eliminated. This showed that the larger k values obtained in compression using uncorrected data were an artifact of the pseudoelastic effect. The apparent friction stress varied between about 14 MPa for pure Mg to very low or negative values for the most dilute alloy, increasing again to about 8 MPa for the most concentrated alloy. The use of strength data corrected for pseudoelasticity effects is necessary for a consistent analysis of the grain size hardening.

DOI: 10.1007/s11661-010-0599-2

I. INTRODUCTION

THE Hall–Petch (H-P) equation[1–4] takes the form

$$\sigma_y = \sigma_o + kd^{-1/2} \quad [1]$$

where d is the grain size and σ_y is the yield strength. The term σ_o is usually interpreted as a friction stress suitably modified by the Taylor factor and k as a stress intensity factor related to the difficulty in transferring slip from grain to grain and to the nucleation of multiple slip within grains.[5,6]

Experiments show that Eq. [1] describes the relationship between the strength and grain size in both cubic and hexagonal metals.[7–11] However, in the case of Mg and its alloys, the literature[11–15] shows large discrepancies in the values of both σ_o and k. There are several reasons that may account for the apparently contradictory observations from different laboratories in pure Mg[7,9] and its alloys.[16–18] First, the strong dependence of both parameters on orientation texture affects σ_o and k in opposite directions.[9,19] Second, both parameters depend on the deformation mode (slip or twinning) and, therefore, on the proportions of each,[20–23] this being especially important in pure Mg.[24–26] Third, the strain at which the yield strength is determined[10,27,28] can depend on the individual investigator. Fourth, solid solution effects on both σ_o and k are important and are yet to be quantified, as explained in more detail below.

Solid solution effects on the strength of Mg are anisotropic;[29] in dilute Mg-Zn and Mg-Al alloys, solute atoms harden the basal plane,[30–32] whereas they cause solid solution softening of the prism and pyramidal slip systems.[33–35] In concentrated Mg-Zn alloys (c = 0.5 to 2.6 at. pct, where c is the solute concentration), Zn causes extensive hardening, which has been ascribed to short-range order.[32]

Extension {10-12} twins are preferentially activated at low strains in compression[25,29] creating a tension/compression (t/c) asymmetry in the yielding behavior, which may be quite pronounced in the presence of intense basal texture[13,36] although less so in random polycrystals.[29] The twinning stress in Mg and its alloys appears to have a stronger dependence on grain size than does yield by dislocation slip,[13,21–23] as it does in other face-centered cubic, body-centered cubic, and hexagonal metals.[20,37–39] A larger k value should, therefore, be expected whenever twinning dominates, in particular for large grain sizes and in compression, whereas, for small grain sizes, typically below ~30 μm, a reduced k should be expected.[13,22] An opposite view is held by Jain *et al.*[18] who argue that since slip precedes twinning, twinning should not have a direct effect on k, at least in tensile deformation and as long as dislocation plasticity is the dominant deformation mechanism. The presence of solute increases the activation stress for twinning[24] more than for slip; therefore, any twinning effects on the yielding behavior are expected to be less intense for the alloys[25] than for the pure metal.

In-situ neutron diffraction studies in pure Mg and Mg-Al alloys,[40,41] cyclically loaded and unloaded, showed that many of the {10-12} extension twins formed during straining are elastic and partly revert upon unloading. Keshavarz and Barnett[42] also showed that many grains that do not twin during the loading cycle do twin upon

C.H. CACERES, Reader in Casting Technology, is with the ARC Centre of Excellence for Design in Light Metals, Materials Engineering, School of Engineering, The University of Queensland, Brisbane, QLD 4072, Australia. Contact e-mail: c.caceres@uq.edu.au GEMMA E. MANN, formerly Postgraduate Student, CAST Co-operative Research Centre, Materials Engineering, School of Engineering, The University of Queensland, is now Lecturer with Central Queensland University, Rockhampton, QLD 4701, Australia. J.R. GRIFFITHS, Post-Retirement Fellow, is with CSIRO Process Science and Engineering, Kenmore, QLD 4069, Australia.
Manuscript submitted May 14, 2010.
Article published online January 11, 2011

unloading. The overall effect is a pronounced pseudoelastic strain and large hysteresis loops upon loading-unloading.[25,40,42–44] The pseudoelastic effect is larger in pure Mg, in compression, and for small grain sizes.[25,40,43] Aluminum in solution causes a mild decrease of the pseudoelastic effect, whereas Zn causes a far larger decrease.[25,43] The pseudoelastic strain adds to the total strain as the material is loaded, introducing a systematic error in the offset strain at which the strength is measured[45] and, hence, upon the H-P parameters.[26]

The H-P parameters of Mg alloys may thus depend on the loading direction (because of the t/c asymmetry), the solute concentration (because of the anisotropy of the solid solution effects), and the prior thermomechanical history (because of texture effects). In addition, the measurement of the yield strength may be affected systematically by the pseudoelasticity stemming from elastic twinning: (a) for small grain sizes, a transition from twinning-dominated to slip-dominated deformation can be expected; and (b) solute in solution is also expected to decrease the incidence of twinning at low strains in comparison with the pure metal. None of these important effects on the H-P relationship of Mg and its alloys has yet been quantified.

The present work examines the solute dependence of the H-P constants in cast (orientation texture-free) Mg and Mg-Zn alloys, in tension and compression, accounting for pseudoelasticity effects. The Zn contents cover both dilute ($c < 0.5$ at. pct Zn) and concentrated (up to 2.3 at. pct Zn) solid solutions. Magnesium-zinc alloys were selected for the study as they can be grain refined by chemical means, using Zr, without having to use strain-anneal methods, which are known to introduce orientation textures.[9] This method carries two undesirable side effects. First, an unknown solid solution effect will exist, especially in pure Mg, through the formation of Zr-rich cores.[46] Second, as the smallest grain size that can be practically achieved with this method is only ~20 μm, the range of grain sizes that can be explored is somewhat limited.

II. EXPERIMENTAL DETAILS

A. *Materials*

Magnesium of commercial purity was melted in an electric furnace and Zn was added to produce target alloy compositions of 0.4, 0.8, and 2.3 at pct Zn (1, 2, and 6 wt pct Zn respectively). Predetermined amounts of a Mg-25 wt pct Zr master alloy were added to the liquid to produce four different grain sizes for each Zn content. The grain refining effect of Zr depends on the presence of evenly distributed insoluble particles throughout the melt.[47,48] Thus, the melts were mechanically stirred for several minutes prior to casting to maximize the dissolution of Zr while evenly distributing the remaining (insoluble) Zr particles. Pouring was done at 1053 K (780 °C) into sand molds to produce plates measuring 175 × 150 × 33 mm. To further reduce the grain size through increased solidification rate, several castings were made in small cylindrical steel molds, preheated to 473 K (200 °C). The cylindrical castings were either 70 mm in diameter and ~150 mm tall or 20 mm in diameter and ~130 mm tall.

The compositions of the castings were determined by inductively coupled plasma atomic emission spectrometry, and the amounts of soluble and insoluble Zr were determined using the method of Qian *et al.*[48] These compositions, the grain sizes, and the identification keys to the alloys are listed in Table I.

Solution heat-treatments of the cast plates and cylinders were done at different temperatures to follow the solidus line in the Mg-Zn phase diagram, as recommended by Lagowski and Meier,[49] with the extended times for the more concentrated alloys used by Blake and Cáceres[50] and Mann *et al.*[27] The Mg-0.4Zn and Mg-0.8Zn alloys were solution treated at 793 K (520 °C) for 3 hours, and the Mg-2.3Zn alloy was solution treated at 723 K (450 °C) for 9 hours, after which the specimens were quenched in water. Longitudinal sections of the heat-treated cast plates were polished and etched to reveal the grain structure. The grain size was measured by a linear intercept method, and no corrections were applied to obtain the true grain size.

The flow curves of fine-grained pure Mg of earlier experiments by Andersson *et al.*[11] were also used for the analysis. The grain size of the pure Mg used in these experiments was reassessed on the original specimens using

Table I. Chemical Composition, Casting Method (Permanent Mold (PM) or Sand Mold (SM)), Grain Size, and Identification Key to the Alloys Studied; for the Determination of Soluble and Insoluble Zr, See Ref. 48

Zn (at. pct)	Zr Total/ Soluble (at. pct)	Grain Size (μm)	Casting Method	Key
0*	0.36/—	19	PM	Mg
0	0.18/0.12	37	PM	Mg
0	0.22/0.12	40	PM	Mg
0	0.17/0.12	91	SM	Mg
0	0.0008/0	670	SM	Mg
0	0.01/0.002	747	SM	Mg
0	0.001/0	1440	SM	Mg
0.37	0.17/0.07	30	PM	0.4
0.37	0.26/0.09	39	PM	0.4
0.38	0.32/0.10	60	SM	0.4
0.31	0.01/0.005	150	SM	0.4
0.36	0/0	211	SM	0.4
0.32	0.02/0.006	245	SM	0.4
0.70	0.16/0.002	25	PM	0.8
0.66	0.34/0.08	41	PM	0.8
0.84	0.20/—	65	SM	0.8
0.76	0.05/0.04	163	SM	0.8
0.71	0.01/0.008	305	SM	0.8
0.82	0/0	375	SM	0.8
2.29	0.16/0.09	46	PM	2.3
2.10	0.31/0.13	48	PM	2.3
2.11	0.27/0.07	81	SM	2.3
2.13	0/0	197	SM	2.3
2.10	0.008/0.003	344	SM	2.3
2.18	0/0	500	SM	2.3

*This set of specimens was from earlier work by Andersson *et al.*[11]

both linear intercept and electron backscatter diffraction after noting a discrepancy with the published data.*

*The original publication[11] reports the grain size for this material as 36 μm, whereas the present measurements yielded 19 μm.

B. *Mechanical Testing*

Cylindrical tensile specimens with a gage length of 40 mm were machined from the cast plates. The gage diameters were varied from 6 to 24 mm to ensure a ratio of gage diameter to grain size, D/d, above 35.[6] For compression testing, cylindrical specimens were used with gage length 40 mm and diameter 20 mm, ensuring that $D/d \geq 40$ applied for all materials, except for the two or three coarsest grain-sized pure Mg samples (Table I).

Monotonic tension and compression testing was performed on about half of the specimens, for all grain sizes and compositions, at a crosshead speed of 0.7 mm/min. Tensile testing was continued to fracture, whereas compression was usually stopped at about 4 pct. In order to measure the pseudoelastic strain, the rest of the specimens were subjected to a procedure of cyclic loading-unloading at predetermined strains along the flow curve, as described elsewhere.[25] For experimental convenience, a crosshead speed of 0.01 mm/min was used for unloading at very low strains, switching to 0.7 mm/min at strains >1 pct; no strain rate effects could be detected to invalidate this procedure. More than 300 specimens were tested in the experiments, with an average of ~70 data points per alloy for the H-P plots and a minimum of 21 points for alloy 2.3 tested in compression.

Strain was measured using an averaging system composed of two identical extensometers on opposite sides of the specimen. This arrangement compensates for bending strains caused by misalignments of the load train. A sampling rate of 250 s^{-1} was imposed on the analog-to-digital converters to average out the noise from the servohydraulic system while preserving the resolution in load and strain. Carefully aligned, hydraulically controlled collet grips were used to further ensure uniaxial loading during the tensile tests. Compressive testing was done between platens with curved seats that were aligned to be parallel by closing the platens together and loading before tightening into place. This overall setup enabled measurements to be made at strains as low as ~4×10^{-5}.

III. RESULTS

A. *Grain Microstructure*

The mean grain size at different positions in the cast plates was constant to within ±30 pct for any of the large-grained pure Mg castings, and within ±15 pct for the rest of the materials. The mean values of the grain sizes of similarly cast plates differed by less than 10 pct. The grain microstructure was equiaxed and uniform for the finer grain sizes, especially for the alloys, as shown by Figure 1(a), but it was increasingly less uniform for the largest grain sizes. The coarsest-grained pure Mg developed columnar grains, as shown in Figure 1(b). The specimens in these cases were machined from the center of the plates to avoid the columnar grains as much as possible, as indicated in Figure 1(b) by the circle representing the tensile specimen gage diameter.

Since texture strongly affects the yield strength of these alloys, it is important to verify that the castings have a random or near-random texture. This is, for example, clearly not the case for the columnar grain region at the edges of the pure Mg castings (Figure 1(b)). Four samples were chosen for a texture analysis: pure Mg and the Mg-2.3Zn alloy, both with the finest and coarsest grain sizes. Texture was assessed by measuring the {0002} pole figures using X-ray diffraction, and these did not reveal any preferred alignment of crystallographic orientation.

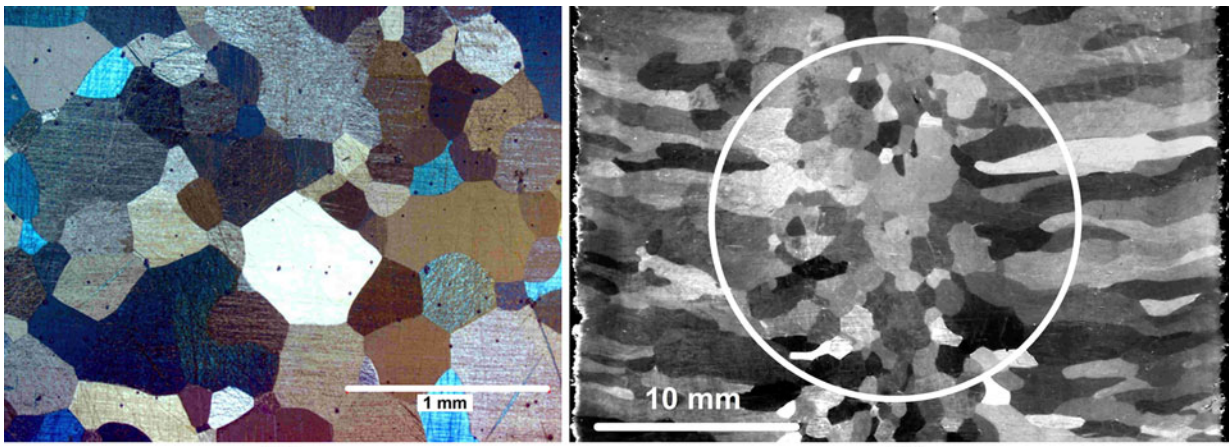

Fig. 1—(*a*) Grain structure in alloy 0.8Zn (grain size = 305 μm); (*b*) macro photograph of pure Mg. The circle indicates the location of the tensile specimens cross section (gage diameter = 18 mm) machined from the plate (grain size inside the circle = 747 μm).

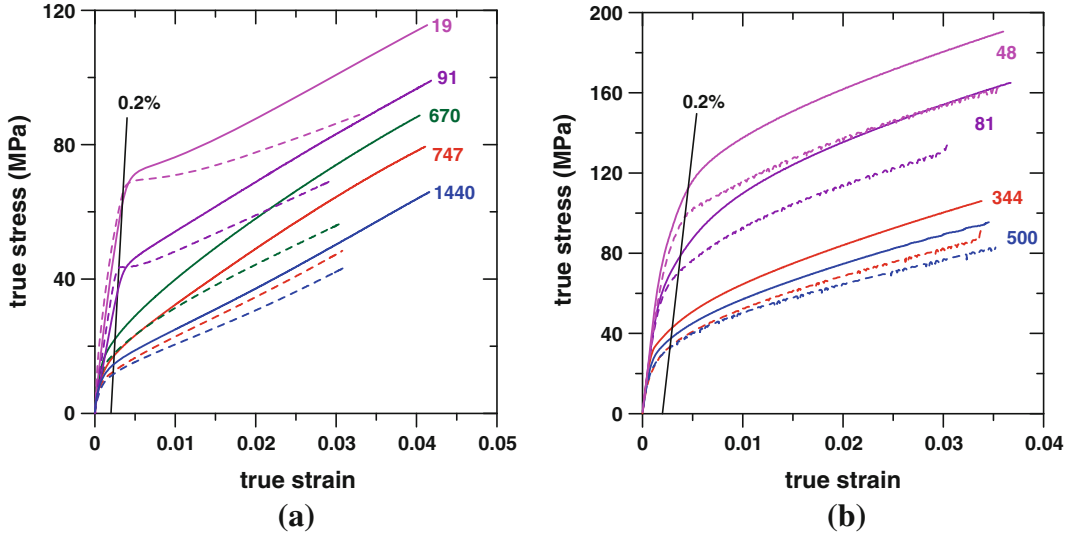

Fig. 2—Tensile (solid lines) and compressive (dashed lines) flow curves for (*a*) pure Mg; (*b*) alloy 2.3Zn. The 0.2% offset strain is indicated by a straight line with gradient 44 GPa. The numerals next to each curve are the grain sizes in μm. The flow curves for the 19 μm specimens in (a) are from Ref. 11. Note that Fig. 6 shows the specimen-to-specimen variation at constant grain size.

B. *Mechanical Testing*

The grain size strengthening in pure Mg and alloy 2.3Zn, in tension and compression, is illustrated by the flow curves of Figures 2(a) and (b), respectively, and Figure 3 shows the effect of solute concentration at (nearly) constant grain size. Significant scatter was encountered in the strength at large grain sizes in all of the compositions studied, which accounted for most of the dispersion of results in the H-P plots described later. The reasons for this inconsistency are thought to lie with the non-uniformity of grain size within the cast plates and, in the case of pure Mg, with the presence of columnar grains.

Figure 4(a) is a monotonic tensile loading curve, followed by one full unloading-loading cycle, for a pure Mg specimen, illustrating the pseudoelastic strain created by elastic twinning. The initial loading slope here and in all experiments was close to 44 GPa, but this only held for applied stresses of less than a few MPa, above which "preyield" microstrain was evident. Figure 4(b) shows that the strain hardening rate at low strains increases, and the amount of pseudoelastic strain decreases, with the Zn content. (The meaning of the thin dashed lines in Figures 4(a) and (b) is explained in relation to Figure 7 and the permanent set strength data.)

Figure 5 shows the relationship between the pseudoelastic strain and the (unloaded) permanent strain (*i.e.*, the plastic strain) for pure Mg in compression, for different grain sizes, and for fine-grained alloy 2.3Zn. Note that for small-grained Mg, the pseudoelastic strain is generally larger than the permanent (unloaded) strain. Prior studies of the pseudoelastic effect in the materials of this work[25] and in alloy AZ91[43] show that for given compositions and for the smaller grain sizes, pseudoelasticity is more marked in compression and tends to develop later in strain as the solute content increases.

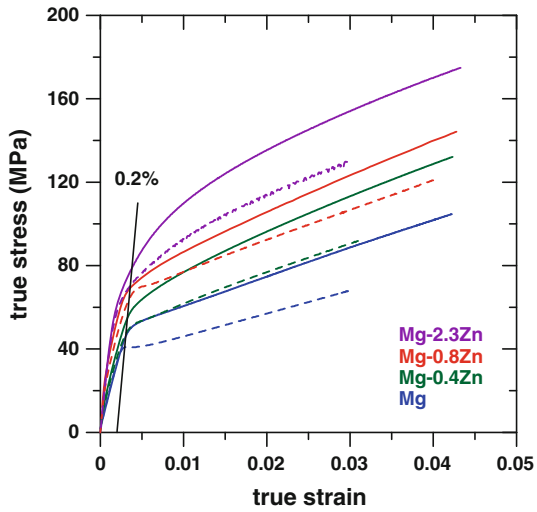

Fig. 3—Effect of increased Zn on the flow behavior at near constant grain size. Grain sizes: Mg: 91 μm; 0.4Zn: 60 μm; 0.8Zn: 65 μm; 2.3Zn: 81 μm. Figure 6 shows the specimen-to-specimen variation in strength at constant grain size.

C. *H-P Plots Using On-Load Proof Stress Data*

The on-load 0.2 pct proof stress was determined in tension and compression. Here, "on-load" means that 0.2 pct is the sum of the plastic and anelastic strains (Reference 45, Section 13.1 and Figure 6). The data are plotted as H-P graphs (termed "Ordinary Hall–Petch plots") in Figure 6(a) for pure Mg and Figure 6(b) for all materials. The lines of (least-squares) best fit to the different sets of data resulted in the values listed in Table II, with the apparent friction stress, σ_o, determined as the ordinate intercept, and k as the corresponding slope. Figure 6(a) includes tensile data for pure Mg from Hauser *et al.*[51] (solid circles). The

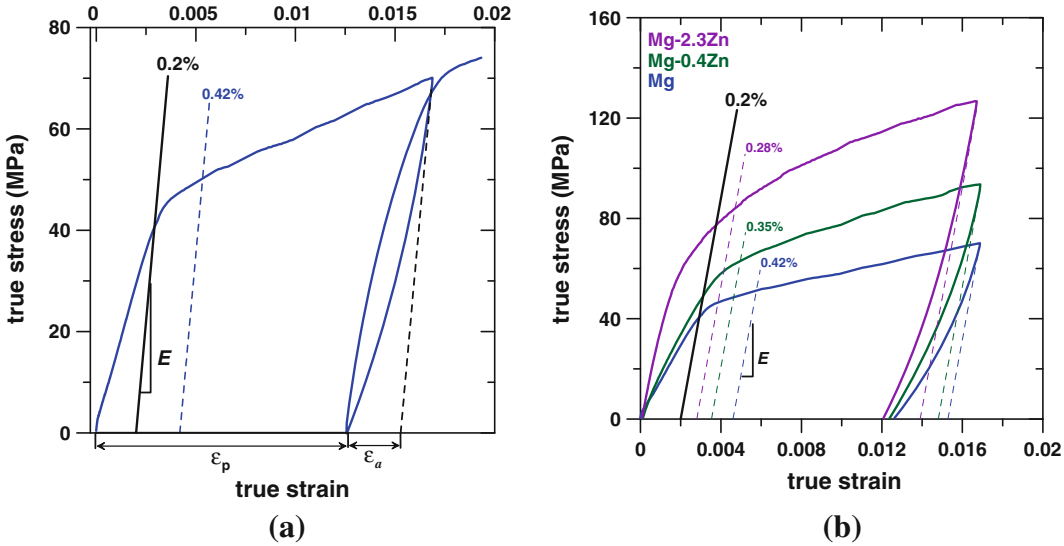

Fig. 4—(*a*) Tensile loading, followed by unloading-loading, for pure Mg, showing the magnitude of the pseudoelastic strain. ε_p and ε_a indicate the permanent plastic and pseudoelastic strains, respectively; (*b*) the pseudoelastic effect for different Zn contents, under tensile deformation. The thin dashed lines indicate the offset strains used to determine the permanent set strength (see text). The numeral next to each dashed line indicates the offset strain corrected for pseudoelasticity. Grain sizes: Mg: 91 μm; 0.4Zn: 60 μm; 2.3Zn: 81 μm.

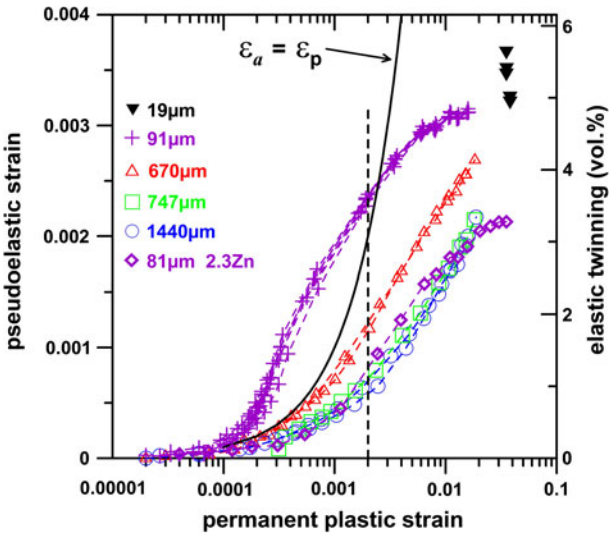

Fig. 5—The pseudoelastic strain (ε_a, defined in Fig. 4(a)) as a function of the permanent plastic strain (ε_p), for pure Mg of different grain sizes and small grained alloy 2.3Zn, all tested in compression. The solid line indicates when the two strains are the same. The solid down triangles on the upper right corner (19 μm) correspond to Andersson *et al.*'s specimens.[11] The dashed vertical line indicates the 0.2% offset permanent strain. The right y-axis is the calculated amount of elastic twinning (see Section IV).

present set of data and those of Hauser *et al.* are remarkably consistent with each other (as are the respective k and σ_o values). Note that Hauser *et al.*'s material was grain refined by a strain anneal method (*i.e.*, without using Zr).**

**Wilson and Chapman[9,19] compared Hauser *et al.*'s data with their own obtained with heavily textured Mg and concluded that the former had only a weak orientation texture.

D. *Hall-Petch Plots Corrected for Pseudoelasticity*

Figure 2 shows that for large grain sizes, at the 0.2 pct offset strain, the specimens are already well into generalized plastic deformation, whereas for small grain sizes, the strength is measured in the high strain hardening region to the left of the "knee" in the flow curve. This inconsistency of the standard 0.2 pct offset strain method for measuring the strength of Mg has already been pointed out by Andersson *et al.*[11] Mann *et al.*[26] argued that this inconsistency is largely caused by pseudoelasticity effects and can be eliminated when the procedures illustrated in Figures 4 and 7 are applied.

Figure 4 shows that upon unloading, as the pseudoelastic effect reverts to zero, the true (unloaded) permanent plastic deformation can be measured. Thus, specimens of each grain size and Zn content were cyclically loaded and unloaded at increasing strains, and plots of stress *vs* (unloaded) true plastic strain were constructed, as shown in Figure 7. It is noted in passing that this procedure is a more exact version of that recommended in the ISO Standard for tensile testing.[45]

The correction described in Figure 7 was applied to the specimens for which loading/unloading data were collected (about half of all specimens of this study) as part of a prior study on pseudoelasticy.[25] The rest of the specimens were deformed monotonically, and data for the pseudoelastic strain were not obtained. To correct the strength data for the pseudoelastic strain in the monotonic specimens, average values for the pseudoelastic component at the 0.2 pct permanent plastic strain, read from Figure 5 or similar plots previously published,[25] were added to the nominal offset strain to obtain a true permanent (0.2 pct) offset strain. Offset strains thus corrected are shown in Figures 4(a) and (b).

Figures 4 and 7 show that once corrected for pseudoelasticity the yield strength is measured well into the

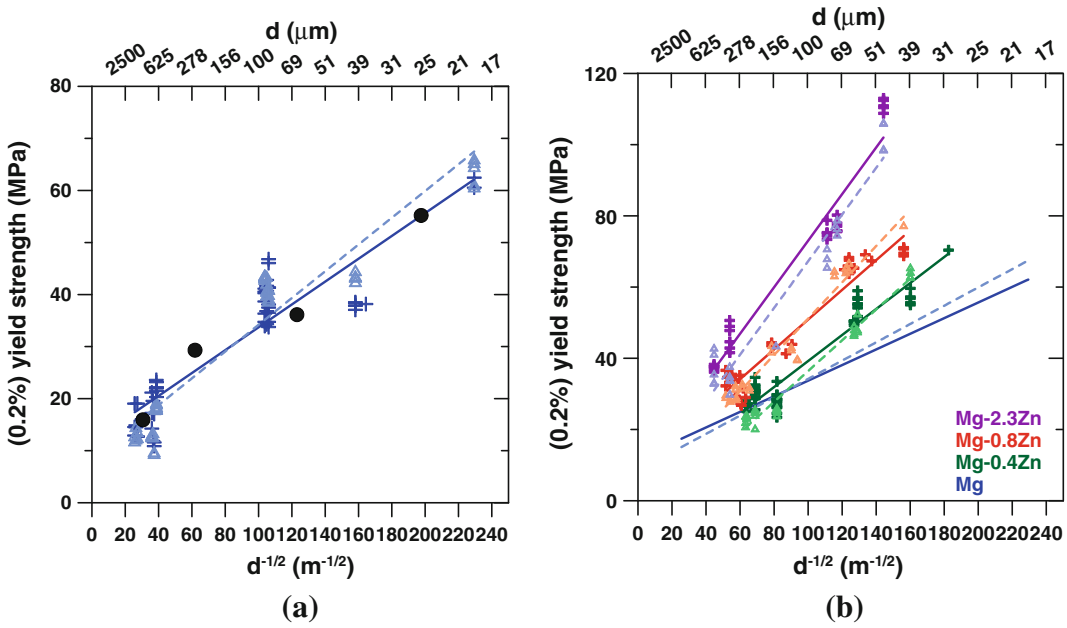

Fig. 6—Ordinary Hall–Petch plots for (*a*) pure Mg; (*b*) all materials. For clarity the pure Mg data points have been removed from (b). In these and the H-P plots of Fig. 8 the crosses and solid lines denote tensile data, the triangles and dashed lines denote compression. The solid circles in (a) are tensile data from Hauser *et al.*[51] See Table II for the numerical values of the Hall–Petch parameters.

Table II. Ordinary Hall–Petch Constants Using (0.2 pct On-Load Offset Strain) Strength Values, Determined from the Lines of Best Fit of Fig. 6; the Error Given Corresponds to One Standard Deviation of This Fit

Alloy	Testing Direction	σ_o (MPa)	k (MPa m$^{1/2}$)
Mg	tension	11.8 ± 1.4	0.22 ± 0.01
	comp.	8.5 ± 1.5	0.26 ± 0.01
Mg-0.4Zn	tension	2.7 ± 1.9	0.37 ± 0.02
	comp.	–6.8 ± 1.4	0.43 ± 0.01
Mg-0.8Zn	tension	9.1 ± 2.2	0.42 ± 0.02
	comp.	0.2 ± 2.1	0.51 ± 0.02
Mg-2.3Zn	tension	7.7 ± 3.0	0.65 ± 0.03
	comp.	1.7 ± 3.5	0.66 ± 0.04

regime of general plastic deformation for all materials (*i.e.*, past the knee in the flow curve). The correction for pseudoelasticity is more important for small grain sizes and for the pure metal, as anticipated from Figure 5. The flow stress data corrected for pseudoelasticity were used to create the graphs of Figure 8, termed "permanent set strength" H-P plots; the parameters of best fit to Figure 8 are listed in Table III.

The permanent set k values are larger than for the ordinary H-P data of Table II by, on average, 0.05 MPa m$^{1/2}$. This difference is relatively more significant for the pure Mg and the more dilute alloys; more importantly, the values for tension and compression are now very close to each other and do not show the systematic t/c bias evident in Table II. This suggests that the higher k values obtained in compression using the ordinary H-P plots are largely an artifact created by the pseudoelastic strain being larger for the pure Mg and the lower alloys, for smaller grain sizes and in compression (Figure 5).

The σ_o and k values of Tables II and III are plotted in Figures 9 and 10, respectively, as a function of the Zn content. Figure 9 shows that that the friction stress goes through a narrow minimum at 0.4 at. pct Zn, and for the higher alloys, it remains generally lower than for the pure Mg. As the alloys are stronger than the pure metal in both tension and compression (Figure 3), it is odd that their friction stresses should be lower. Note, too, that the apparent friction stress is lower for compression loading for Mg and the Mg-Zn alloys. Figure 10 shows that k increases monotonically with the solute content, rapidly for the lower concentrations, and then more slowly, both for the ordinary and permanent set strength data.

IV. DISCUSSION

A. *Scatter of Experimental Data*

The most irritating experimental issue affecting the present sets of data is the inconsistency of the grain size strengthening, particularly at large grain sizes. Possible reasons for the scatter in strength are the presence of Zr-rich cores, the free surface effects, the relatively large dispersion of grain sizes around the average value (±30 pct for large-grained pure Mg and ±15 pct for the rest), and the columnar grains in large-grained pure Mg.

1. *Effect of Zr*

The mean concentration of Zr in solution varied from zero (for the coarsest grain sizes) to 0.13 at. pct (for the finest grain sizes). This low concentration should have

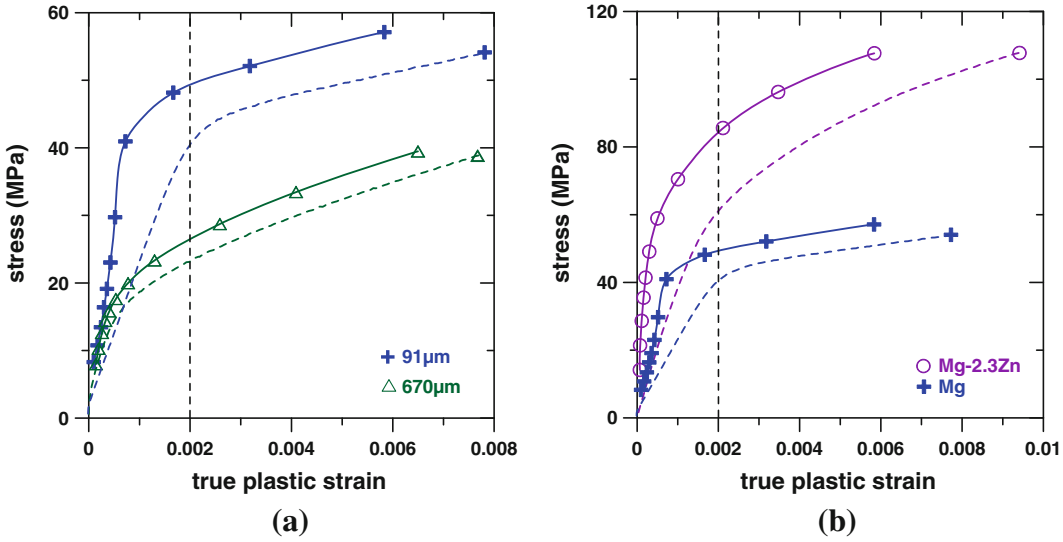

Fig. 7—Flow curves before and after correcting for pseudoelastic effects. The dashed lines are monotonic tensile flow curves, the solid lines are the corresponding curves after subtracting the pseudoelastic strain from the total strain. (*a*) Pure Mg at two grain sizes; (*b*) pure Mg (grain size = 91 μm) and alloy 2.3Zn (grain size = 81 μm). The symbols on the solid lines identify the points where the pseudoelastic strain was measured.

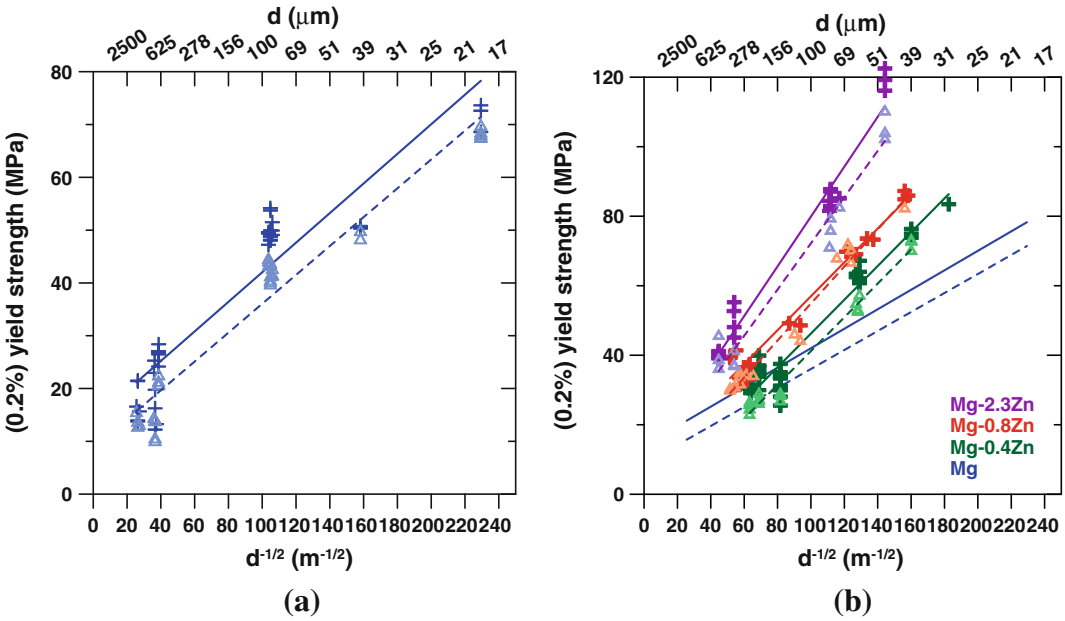

Fig. 8—Hall–Petch plots for the permanent set strength method. (*a*) Pure Mg; (*b*) all materials. The pure Mg data points have been removed for clarity. See Table III for the Hall–Petch parameters.

no significant effect on the yield stress. However, it is known that Zr-rich cores exist in cast Mg-Zr alloys.[46] The concentration of Zr at the center of the cores may be as high as 0.5 at. pct, decreasing to nearly zero some 20 μm away from the nucleating particle. Larger grains may have several cores. The solid solution hardening (or softening) introduced by the Zr is unknown, adding a degree of uncertainty to the data.

2. *Effect of the free surface*

Kocks[6] pointed out that the effect of the grains on the surface of a polycrystal may be, in his words, well nigh impossible to model theoretically. A common arbitrary criterion for measuring true polycrystalline properties is that fewer than 10 pct of the grains should sit on the surface of the specimens, something that can be achieved by making the specimen diameter-to-grain size ratio >30. In the present experiments, this ratio was >35 for the tensile specimens and >40 in all the compression specimens, except for the coarsest-grained pure Mg (Table I). The plastic anisotropy of Mg is likely to ensure that grains near or on the surface deform by basal slip even with extremely low Schmid factors, exacerbating any free surface effects in large-grained specimens, and it may be the case that a specimen diameter/grain size ratio of 35 is too small for Mg.

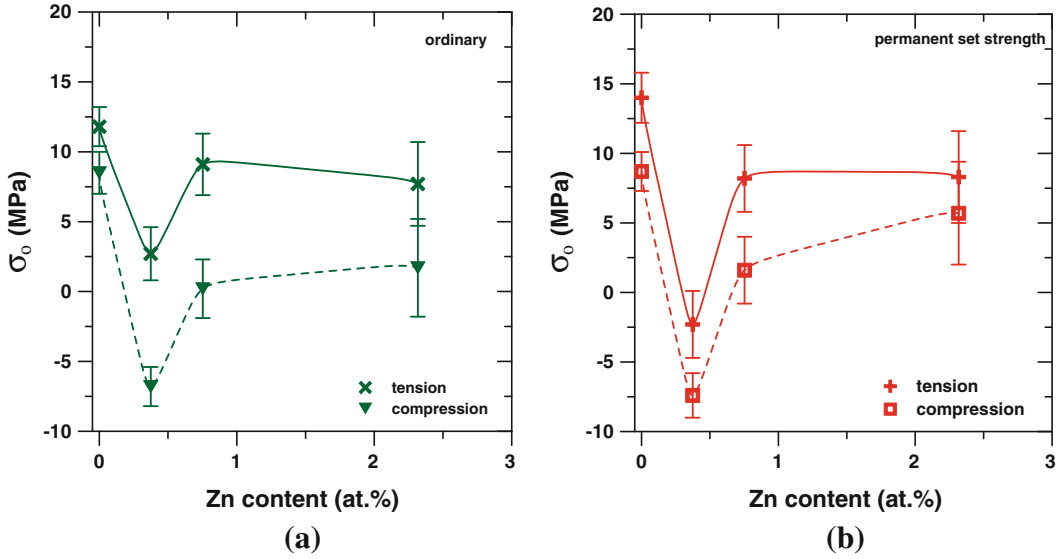

Fig. 9—The apparent friction stresses, σ_0, derived from (*a*) the ordinary Hall–Petch plot; (*b*) the permanent set strength plot (Tables II and III, respectively). The error bars indicate one standard deviation.

Table III. Hall–Petch Constants Using Permanent Set Strength Values (Strain Corrected for Pseudoelasticity), Determined from the Lines of Best Fit of Fig. 8; the Error Given Corresponds to One Standard Deviation of This Fit

Alloy	Testing Direction	σ_o (MPa)	k (MPa m$^{1/2}$)
Mg	tension	14.0 ± 1.8	0.28 ± 0.02
	comp.	8.7 ± 1.4	0.27 ± 0.01
Mg-0.4Zn	tension	–2.3 ± 2.4	0.49 ± 0.02
	comp.	–7.4 ± 1.6	0.49 ± 0.02
Mg-0.8Zn	tension	8.2 ± 2.4	0.49 ± 0.02
	comp.	1.6 ± 2.4	0.53 ± 0.03
Mg-2.3Zn	tension	8.3 ± 3.3	0.72 ± 0.03
	comp.	5.7 ± 3.7	0.67 ± 0.04

3. *Effects of grain size distribution and texture*

With regard to the large dispersion of grain sizes, it may be tempting to suggest that the scatter in the strength data in the H-P plots is associated with a either a bimodal size distribution or mild texture effects. Bimodal distributions are common in high-pressure diecast Mg alloys[52,53] and are sometimes observed in recrystallized wrought Mg alloys,[54] but there was no obvious evidence for bimodality in our castings (except for the large-grained pure Mg). As noted in Section III–A, no evidence could be found of texture in any of the castings.

Two points can be made to assert that these several effects (*A*1 to *A*3) are minor. First, there is a near-perfect match of our data with those of Hauser *et al.*[51] (solid circles in Figure 6(a)), which lacked both Zr coring and columnar grain effects. Second, the scatter of data in these experiments was much smaller than that reported by others,[11,18,55] most likely because of the large diameter/grain size ratio used in the test specimens.

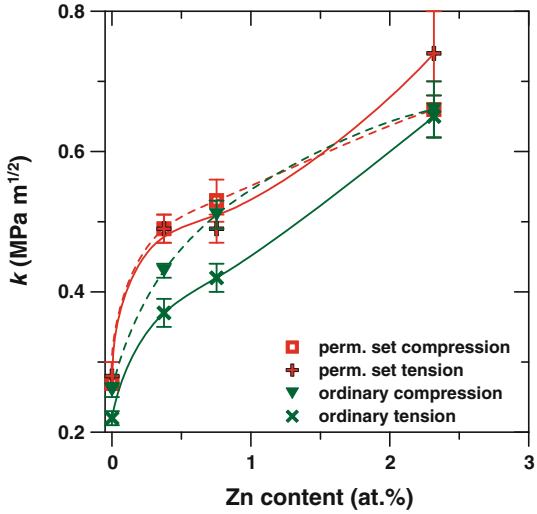

Fig. 10—Stress intensity factors, k, for the alloys (Tables II and III) studied. The error bars indicate one standard deviation.

B. *Twinning Effects on k*

The right-hand y-axis of Figure 5 represents the volume fraction of elastic twinning, f_{et}, that would produce a given amount of pseudoelastic strain, ε_a, calculated as[56] $f_{et} = m(\varepsilon_a/\varepsilon_t)$, where m is the Schmid factor (taken as 0.5 for a random polycrystal) and $\varepsilon_t = 0.13$ is the {10-12} twinning shear strain. Figure 5 shows that at the 0.2 pct offset strain and for a given grain size, f_{et} in the pure Mg is several times larger than for the 2.3Zn alloy. The predicted volume fraction of elastic twins at the 0.2 pct offset strain ranges from 1 pct for the 2.3Zn alloy to 4 pct for the pure Mg. No attempt was made in these experiments to measure the actual volume fraction of elastic twins which, by necessity, can only be a fraction of the total amount of twinning.[25,40,43] However, the calculated amount of elastic

twinning at yield for the 2.3Zn alloy (f_{et} ~1 pct) appears consistent with SEM observations by Keshavarz and Barnett[42] in alloy AZ31, which indicate that at 1 pct strain, twins cover an area fraction between 2 and 6 pct.

Barnett[21] suggested that a transition in the dominant deformation mechanism, from twinning at large grain size to slip at small grain size, should occur. Such a transition implies a decreased k value for small grain sizes, and experiments in very fine-grained alloy AZ31 appeared to support this hypothesis.[13,22] In the present case, the material that exhibited the largest tendency to twin was pure Mg, and the twin/slip transition in k should be most evident in the ordinary H-P plot of Figure 6(a). The data do not support the idea of a transition and nor for that matter do any of the alloys in Figure 6(b). Jain *et al.*[18] showed that the volume fraction of twinned material in AZ31 is only mildly dependent on grain size for grain sizes above 30 to 40 μm. In addition, these authors argued that as long as dislocation plasticity precedes twinning, the latter should not have a direct effect on k. The fact that correcting for pseudoelasticity eliminated the difference in k values between tension and compression also seems to support this view. It thus appears that the slip/twin transition is only evident at finer grain sizes than we have been able to produce.

C. *Solute Effects on σ_o and k*

The behavior of the friction stress in Figures 9(a) and (b) is puzzling. The alloys exhibit a smaller apparent friction stress than pure Mg, contrary to what can be expected from the overall increase in the alloy strength with solute content (Figure 3). It may be argued that the friction stress reflects the solid solution softening effects on prism slip,[57] but specific data are required to elucidate this point. Figure 9 shows that the apparent friction stress is negative for the dilute alloy and this is not physically meaningful. Similar behavior has been noted for ordered Ni_3Al,[58] and in both that work and ours, it must be concluded that the H-P paradigm does not always apply for very large grain sizes. It is noteworthy that Ni_3Al had a much higher k value in the ordered state than in the disordered one, in keeping with other Ll_2 structures.[7,59]

The monotonic increase in the k values with the Zn content exhibited by the data in Figure 10 is broadly consistent with the notion that any form of hardening that restricts multiple slip, particularly long-[7,59] or short-range order,[8,60] should increase the k value for the concentrated alloys. On the other hand, the data in Figure 10 do not reflect the solid solution softening effects of the dilute alloys,[33] which, by making prism slip easier, can be expected to decrease the k value of the more dilute alloy[57] in comparison with pure Mg. Since twinning is more prevalent at low strains in pure Mg than in the alloys,[24] it is speculated that profuse twinning may account for the low k value of the pure metal. Likewise, this is an aspect that requires further work. We note that Gd has a strong solid solution strengthening effect on Mg, comparable with that of Zn.[61,62] Small angle X-ray diffraction studies[63] have shown that Mg-Gd alloys develop short-range order, as is also likely in Mg-Zn alloys,[32] and we suggest that the solute concentration effects on k are likely to be as high in Mg-Gd as they are in Mg-Zn.

By and large, the present results show that all prior work on H-P effects in Mg, using ordinary H-P plots, has very likely underestimated the actual k values because of the systematic errors in the measurement of the yield strength caused by the pseudoelastic effect, especially for the pure Mg and the leaner alloys. This criticism applies to earlier work by the present authors[11,27] as much as those of others. These errors can be avoided by using permanent set strength data determined with the methods described in this work. Once the correction for pseudoelasticity is applied, the measurement of the strength is consistent across the range of grain sizes and solute contents; in particular, correct (larger) k values are obtained and the difference between tension and compression is eliminated.

V. CONCLUSIONS

The following conclusions can be drawn from this work:

1. The H-P stress intensity factor, k, obtained using the on-load 0.2 pct offset strength data increased with the concentration of Zn, from ~0.24 MPa $m^{1/2}$ for pure Mg to ~0.66 MPa $m^{1/2}$ for the most concentrated alloy (2.3 at. pct Zn); the k values were generally larger in compression.
2. Correcting flow strength data for pseudoelasticity ensures consistency in the way the strength is measured and drastically reduces the dependence of the k values on the testing direction. After correcting for pseudoelasticity, the k values range from ~0.28 MPa $m^{1/2}$ for pure Mg and ~0.7 MPa $m^{1/2}$ for 2.3 at. pct Zn alloy.
3. The larger k values in compression of the uncorrected strength data appear to be artifacts resulting from the elastic twinning, being more pronounced in pure Mg metal, in compression, and for small grain sizes.
4. The apparent friction stress was generally lower for the alloys than for pure Mg metal and, indeed, for the 0.4Zn alloy, was even slightly negative.
5. An increase in k value associated with a transition from slip to twinning was not seen in these experiments, and it may be that such a transition occurs at finer grain sizes than we were able to access.
6. Scatter of data seems to be inherent to Mg and Mg-Zn alloys, most likely as a manifestation of the plastic anisotropy consequent upon the hcp crystal structure. The use of a specimen diameter/grain size ratio larger than 35 may be necessary for these metals.
7. All prior work on H-P effects in Mg and its alloys using ordinary H-P plots based on on-load proof stress data has underestimated the k values because of the systematic errors introduced by the pseudoelastic effect. These errors, which are more significant

for the pure Mg and the less concentrated alloys, can be avoided by using permanent set strength data determined with the methods used in this work.

ACKNOWLEDGMENTS

We are grateful to Drs. M.D. Nave and N. Stanford, Deakin University, for performing and interpreting the texture measurements.

REFERENCES

1. A.H. Cottrell: *AIME Trans*., 1958, vol. 212, pp. 192–203.
2. N.J. Petch: *J. Iron Steel Inst (London)*, 1953, vol. 174, pp. 25–28.
3. E.O. Hall: *Proc. Phys. Soc. (London)*, 1951, vol. 64, pp. 747–52.
4. R. Armstrong, I. Codd, R.M. Douthwaite, and N.J. Petch: *Philos Mag*., 1962, vol. 7, pp. 45–58.
5. U.F. Kocks: *Acta Metall*., 1958, vol. 6, pp. 85–94.
6. U.F. Kocks: *Metall. Trans*., 1970, vol. 1, pp. 1121–43.
7. R.W. Armstrong: in *Yield, Flow and Fracture of Polycrystals*, T.N. Baker, ed., Applied Science Publishers, London, 1983, pp. 1–31.
8. J.D. Embury: in *Strengthening Methods in Crystals*, A. Kelly and R.B. Nicholson, eds., Elsevier, London, 1972, pp. 331–402.
9. D.V. Wilson and J.A. Chapman: *Philos Mag*., 1963, vol. 8, pp. 1543–51.
10. N. Hansen: in *Yield, Flow and Fracture of Polycrystals*, T.N. Baker, ed., Applied Science Publishers, London, 1983, pp. 311–50.
11. P. Andersson, C.H. Cáceres, and J. Koike: *Mater. Sci. Forum*, 2003, vols. 419–422, pp. 123–28.
12. C.H. Cáceres, J.R. Griffiths, C.J. Davidson, and C.L. Newton: *Mater. Sci. Eng*., 2002, vol. 325A, pp. 344–55.
13. M.R. Barnett, Z. Keshavarz, A.G. Beer, and D. Atwell: *Acta Mater*., 2004, vol. 52, pp. 5093–103.
14. C.D. Lee: *Mater. Sci. Eng*., 2007, vol. 459A, pp. 355–60.
15. C.H. Cáceres, P. Lukác, and A. Blake: *Philos Mag A,* 2008, vol. 88, http://dx.doi.org/10.1080/14786430701881211, pp. 991–1003.
16. G. Sambasiva Rao and Y.V.R.K. Prasad: *Metall. Trans. A*, 1982, vol. 13A, pp. 2219–26.
17. G. Sambasiva Rao and Y.V.R.K. Prasad: *Scripta Metall*., 1983, vol. 17, pp. 147–51.
18. A. Jain, O. Duygulu, D.W. Brown, C.N. Tomé, and S.R. Agnew: *Mater. Sci. Eng. A*, 2008, vol. 486, pp. 545–55.
19. D.V. Wilson: *J. Inst. Met*., 1966, vol. 98, pp. 133–43.
20. M.A. Meyers, O. Vöhringer, and V.A. Lubarda: *Acta Mater*., 2001, vol. 49, pp. 4025–39.
21. M.R. Barnett: *Scripta Mater*., 2008, vol. 59, pp. 696–98.
22. J. Koike: *Metall. Mater. Trans. A*, 2005, vol. 36A, pp. 1689–96.
23. L.L. Chang, Y.N. Wang, X. Zhao, and M. Qi: *Mater. Characterization*, 2009, vol. 60, pp. 991–94.
24. E.W. Kelley and W.F. Hosford: *AIME Trans*., 1968, vol. 242, pp. 5–13.
25. G.E. Mann, T. Sumitomo, C.H. Cáceres, and J.R. Griffiths: *Mater. Sci. Eng*., 2007, vol. 456A, pp. 138–46.
26. G.E. Mann, C.H. Cáceres, and J.R. Griffiths: *Magnesium Technology 2007,* Orlando, FL, 2007, R.S. Beals, A.A. Luo, N.R. Neelameggham, and M.O. Pekguleryuz, eds., TMS, Warrendale, PA, 2007, pp. 383–88.
27. G.E. Mann, J.R. Griffiths, and C.H. Cáceres: *J. Alloys Compd*., 2004, vol. 378 (1–2), pp. 188–91.
28. N. Ono, K. Nakamura, and S. Miura: *Mater. Sci. Forum*, 2003, vols. 419–422, pp. 195–200.
29. S.R. Agnew, M.H. Yoo, and C.N. Tomé: *Acta Mater*., 2001, vol. 49, pp. 4277–89.
30. A. Akhtar and E. Teghtsoonian: *Acta Metall*., 1969, vol. 17, pp. 1339–49.
31. A. Akhtar and E. Teghtsoonian: *Philos Mag*., 1972, vol. 25, pp. 897–916.
32. C.H. Cáceres and A. Blake: *Phys. Status Solidi a*, 2002, vol. 194, pp. 147–58.
33. A. Akhtar and E. Teghtsoonian: *Acta Metall*., 1969, vol. 17, pp. 1351–56.
34. S. Ando and H. Tonda: *Mater. Sci. Forum*, 2003, vols. 419–422, pp. 87–92.
35. S. Ando and H. Tonda: *Mater. Trans. (JIM)*, 2000, vol. 41, pp. 1188–91.
36. M.M. Avedesian and H. Baker (eds.): *Magnesium and Magnesium Alloys (ASM Specialty Handbook)*. ASM International, Materials Park, OH, 1999, pp. 7–11.
37. P.J. Worthington and E. Smith: *Acta Metall*., 1966, vol. 14, pp. 35–41.
38. M.J. Marcinkowski and H.A. Lipsitt: *Acta Metall.,* 1962, vol. 10, pp. 95–111; DOI:110.1016/0001-6160(1062)90055-X.
39. R.W. Armstrong and P.J. Worthington: in *Metallurgical Effects at High Strain Rates,* R.W. Rhode, B.M. Butcher, J.R. Holland, and C.H. Karner, eds., Plenum Press, New York, NY, 1973, p. 294.
40. M.A. Gharghouri, G.C. Weatherly, J.D. Embury, and J. Root: *Philos. Mag*., 1999, vol. 79, pp. 1671–96.
41. O. Muránsky, D.G. Carr, P. Sittner, and E.C. Oliver: *Int. J. Plast*., 2009, vol. 25, pp. 1107–27.
42. Z. Keshavarz and M.R. Barnett: *Magnesium Technology 2005*, San Francisco, CA, 2005, N.R. Neelameggham, H.I. Kaplan, and B.R. Powell, eds., TMS, Warrendale, PA, 2005, pp. 171–75.
43. C.H. Cáceres, T. Sumitomo, and M. Veidt: *Acta Mater*., 2003, vol. 51, pp. 6211–18.
44. L. Wu, A. Jain, D.W. Brown, G.M. Stoica, S.R. Agnew, B. Clausen, D.E. Fielden, and P.K. Liaw: *Acta Mater*., 2008, vol. 56, pp. 688–95.
45. International Standard ISO/DIS 6892-1 2009, *Metallic Materials–Tensile Testing—Part 1 Method of Test at Room Temperature*, accessed on Sept. 2009.
46. M. Qian, D.H. StJohn, and M.T. Frost: *Scripta Mater*., 2002, vol. 46, pp. 649–54.
47. M. Qian and D.H. St. John: in *Proc. 6th Int. Conf. Magnesium Alloys and Their Applications*, Wolfsburg, Germany, 2003, K.U. Kainer, ed., DGM, Wiley-VCH, Weinheim, 2003, pp. 706–12.
48. M. Qian, D.H. StJohn, and M.T. Frost: *Mater. Sci. Forum*, 2003, vols. 419–422, pp. 593–98.
49. B. Lagowski and J.W. Meier: *AFS Trans*., 1965, vol. 73, pp. 246–54.
50. A. Blake and C.H. Cáceres: *Magnesium Technology 2005*, San Francisco, CA, 2005, N.R. Neelameggham, H.I. Kaplan, and B.R. Powell, eds., TMS, Warrendale, PA, 2005, pp. 403–07.
51. F.E. Hauser, P.R. Landon, and J.E. Dorn: *AIME Trans*., 1956, vol. 206, pp. 589–93.
52. H.I. Laukli, C.M. Gourlay, and A.K. Dahle: *Metall. Mater. Trans. A*, 2005, vol. 36A, pp. 805–18.
53. C.M. Gourlay, H.I. Laukli, and A.K. Dahle: *Metall. Mater. Trans. A*, 2007, vol. 38A, pp. 1833–44.
54. O. Muránsky, M.R. Barnett, D.G. Carr, S.C. Vogel, and E.C. Oliver: *Acta Mater*., 2010, vol. 58, pp. 1503–17.
55. Y.C. Lee, A.K. Dahle, and D.H. StJohn: in *Magnesium Technology 2000*, Nashville, TN, 2000, H.I. Kaplan, J. Hryn, and B. Clow, eds., TMS, Warrendale, PA, 2000, pp. 211–18.
56. P.G. Partridge: *Metall. Rev*., 1967, vol. 12, pp. 169–94.
57. A.H. Blake and C.H. Cáceres: *Mater. Sci. Eng*., 2008, vols. 483–484, pp. 161–63.
58. E.M. Schulson, T.P. Weihs, D.V. Viens, and I. Baker: *Acta Metall*., 1985, vol. 33, pp. 1587–91.
59. F.R.N. Nabarro and H.L. de Villiers: *The Physics of Creep*, Taylor and Francis, London, 1995.
60. L. Zhao and I. Baker: *Acta Metall. Mater*., 1994, vol. 42, pp. 1953–58.
61. L. Gao, R.S. Chen, and E.H. Han: *J. Alloys Compd*., 2009, vol. 481, pp. 379–84.
62. L. Gao, R.S. Chen, and E.H. Han: *J. Alloys Compd*., 2009, vol. 472, pp. 234–40.
63. D.S. Gencheva, A.A. Katsnel'son, L.L. Rokhlin, V.M. Silonov, and F.A. Khavadzha: *Fiz. Met. Metalloved*., 1981, vol. 51, pp. 788–93.